



ORIGINAL RESEARCH PAPER



USING THE CHEMICAL BATH METHOD TO MAKE CdSe THIN FILMS FOR A PHOTOELECTROCHEMICAL CEL

S. H. Mane

Department of Physics, Dr. Datar, Behere and Joshi College, Chiplun, Dist- Ratnagiri, India.415605

*Correspondence author E-mail: samratmane95@gmail.com

Received: 15 December 2025

Revised: 11 January 2026

Accepted: 27 January 2026

Published: 30 January 2026

DOI: <https://doi.org/10.5281/zenodo.18478698>

Abstract:

This study used a non-aqueous liquid to deposit a thin layer of Cadmium Selenide onto a stainless steel substrate. To produce high-quality films, the different physical preparation parameters and the deposition conditions such as the deposition duration and temperature, chemical species concentrations, pH, mechanical stirring speed, etc. were tuned. The prepared sample was examined for composition and is less smooth, diffusely reflecting, and firmly adhering to the substrate's support. Characterizing the photoelectrochemical cell of the photoelectrodes includes examining current-voltage characteristics in the dark, capacitance-voltage in the dark, barrier-height measurements, power output, photo response, and spectrum response. The junction ideality factor was found to be low for the CdSe composition. The barrier height and flat band potential were found to be 0.181 eV and 710 mV, respectively. The short circuit current, open circuit voltage, conversion efficiency, and fill factor are 141 $\mu\text{A}/\text{cm}^2$, 210 mV, 0.54%, and 43.08%, respectively, according to the power output characteristic. The spectral response shows the highest current measured at 725 nm.

Keywords: CdS Thin Film, CBD Methods, Photoelectrochemical Research, Photoelectrode, Optical And Electrical Characteristics.

1. Introduction

Solar energy utilization will play a vital role in solving the worlds energy needs of the future/1/. The direct conversion of sunlight into electricity by solar cells is likely to be a prime method of the future, assuming that practical economic means of direct conversion modes in that it responds linearly to the flux. There is no inertia to a solar cell system; it immediately produces its output at the level approximate to the solar intensity unlike solar thermal systems that need time to reach operating temperature. Fuel transport and storage problems are eliminated in a photovoltaic power system. But the development of the photovoltaic cells, such as silicon, is hampered by the present cost the materials and fabrication [1]. As an alternative for achieving this solar to

electrical conversion, thin film semiconductor/ liquid junction systems based on the Photoelectrochemical effect are of prime importance [2-9]. Several reviews on semiconductor/ electrolyte interfaces are now available in the literature [3-7, 9] and mechanism of the charge transfer across the electrode / electrolyte interface is now fairly understood. Binaries and pseudobinaries of II-VI group compounds are now becoming focus of intensive research since they exhibit potential as efficient absorber in the visible region of the solar spectrum /4-9/. Recently there has been much interest in the application of n-type cadmium chalcogenides, CdX (X=s, Se or Te), electrodes for construction of the Photoelectrochemical solar cells [4-9].

2. Experimental Details

2.1. Preparation of CdSe Photoelectrode

A 250 ml glass vessel was filled with 10 ml (1M) Cadmium Selenide solution for the deposition. To raise the pH of the reacting solution and enhance the film's adherence to the substrate surface, liquid ammonia and triethanolamine (TEA) were added dropwise. In order to do this, 10 ml (1M) of sodium selenosulphate were added. The final reaction mixture had a pH of 11. The ion concentration volumes of the cadmium selenide were adjusted to maintain the film stoichiometry for each of the materials in this series. By adding twice as much distilled water, the reaction bath's total capacity was increased to 200 ml. After that, the reaction vessel was moved to an oil bath at a constant temperature of 72 °C. A constant speed motor was used to rotate the properly cleaned glass substrates at 70 ± 2 rpm. The substrates were placed on a substrate holder that was specifically made for that purpose. The substrates were taken out of the beaker in 180 minutes. Innovative materials for alternative solar cells, such as those that tackle economic, health, and environmental concerns, follow a similar process. Because of this, the photoelectrochemical process is the most complicated use of this method for solar energy conversion. The semiconductor-electrolyte interface can be used to produce power by photoelectrochemistry, photocatalysis, and photoelectrolysis [10, 11]. The direct conversion of solar energy into electrical energy through a semiconductor–electrolyte interface was initially demonstrated by Gerischer and Eills [12, 13]. Since then, a variety of metals have been used as photoelectrode materials in PEC cells, along with mixed oxides and chalcogenides. The stability and efficiency of photoelectrochemical cells are significantly influenced by the conditions under which the photoelectrode, electrolyte, and experiment are prepared [14]. An appropriate thin film photoelectrode for PEC cells must have low resistance and larger grain size. Because of the large grain size, the thin film's grain boundary area is reduced, resulting in an efficient energy conversion. A low resistivity photoelectrode is required to reduce the series resistance of the PEC cell and, consequently, the short circuit current [15, 16]. Polycrystalline semiconductor film can be utilized without suffering a notable decrease in efficiency. This is due to the precise and intimate contact between the crystalline grains and the liquid electrolyte. Thus, PEC cells provide an affordable chemical technique to store solar energy that was modified to create CdSe thin films.

2.2. Fabrication of photoelectrochemical cell

In this study, a PEC cell was created employing graphite rod covered with CoS as a counter electrode, sulphide polysulphide as an electrolyte, and CdSe thin film as the photoanode. The reference electrode was a saturated calomel electrode. The cell was built using a corning glass cuvette shaped like a "H." One benefit of stability against photoelectrode disintegration is an electrolyte solution [17, 18]. It is composed of an H-shaped glass tube with two arms. A normal glass tube with an inner diameter of 1.5 cm and a length of 7 cm was used to construct the opposite arm of the tube, which was made of hard glass and measured 2.7 cm in diameter and 7 cm in length. This

H-shaped glass container was set within a copper pot that was the right size. The photo electrode was illuminated by a window that measured two centimeters by one centimeter. The formula for the photoelectrochemical cell is p-CdSe|NaOH (1M) + Se (1M) + Na₂S (1M)|C (graphite).

The counter electrode is constructed using a graphite rod that has been sensitized in a concentrated CoS solution for a whole day. A rubber cork sealed the cell and supported the counter and photoelectrode. The active region was lighted for one square centimeter. The remaining portion of the film was covered with epoxy resin.

2.3. Characterization of photo electrochemical cell

To get further insight into the mechanism of charge transfer at the electrode-electrolyte interface, the electrical properties of the PEC cell were examined. I-V and C-V characteristics in the dark, power output characteristics under light, and the built-in potential were all measured. The voltage across the junction was adjusted using a wire-wrapped potentiometer, and the current flowing through it was tracked using a current meter. The same circuit was used to determine the capacitance of the junction. The barrier height was examined using the temperature dependence of reverse saturation current at different temperatures, and the illuminated ideality factor was calculated. We were able to determine each cell's junction ideality by plotting the log I vs V graph. Photoelectrochemical activities were examined under 30 mW/cm² of light irradiation. The illumination's intensity was measured using a Meco Lux Meter. To determine the photoresponse, which in turn produced the light ideality factor, the short circuit current (I_{sc}) and open circuit voltage (V_{oc}) as a function of incoming light intensity were measured for each sample. The spectrum response was determined by tracking the open circuit voltage and short-circuit current as a function of the incoming wavelength (400–1000 nm).

3. Results and Discussion

The efficient conversion of incoming light into electrical energy depends on the photoelectrode's ohmic contact with the substrate. It is called ohmic if the contact is non-injecting and the current-voltage connection is linear in both directions [19]. Consequently, the photoelectrode-substrate interaction of each sample was examined.

3.1. Electrical properties

3.1.1. I-V characteristics in dark

The current-voltage (I-V) characteristics of the PEC have been investigated at 300 K. Dark voltage and dark current were found to have evolved. In relation to the semiconductor electrode, this dark voltage was positively polarized. The dark voltage arises from the difference between the two half-cell potentials of a cell [20]. As the positive polarity toward the thin film increases after junction lighting, the voltage increases in magnitude. The sign of this photovoltage indicates that the conductor CdSe is p-type. The photoelectrode components of the electrolyte are deteriorating when some dark current is present [21]. According to the current study, the symmetry factor for CdSe composition was greater than 0.5, suggesting that the interface is rectifying in nature [22]. The dynamic current-voltage characteristics are shown in Figure 1. The junction ideality factor (n_d) is obtained by plotting log I against voltage (mV), and Figure 2 shows the fluctuation. A linear plot was used to evaluate the junction ideality factor.

3.1.2. C-V characteristics in dark

The C-V characteristics of junctions give important information such as the kind of conductivity, donor density, band bending depletion layer width, band edge positions, and flat band potential (V_{fb}) values. The charge space layer capacitance was measured under reverse biased conditions, and the flat band potential was obtained from the Mott-Schottky plot. For representative samples, Figure 3 shows how C⁻² changes with voltage. Extrapolating

the linear parts of these figures to the voltage axis yields the flat band potentials (V_{fb}). The sign of the flat band potential can be used to determine the type of the material. Our analysis suggests that the CdSe material is p-type.

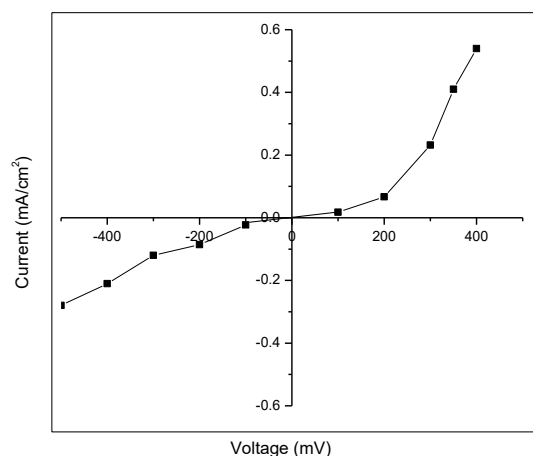


Figure 1: Features of the of CdSe photoelectrode Current - Voltage in dark

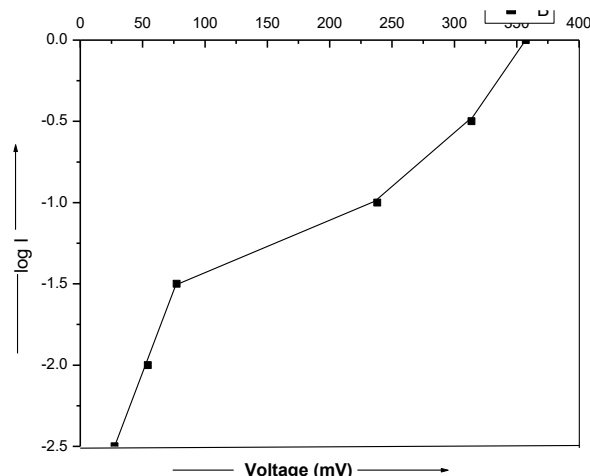


Figure 2: Plot of Log I against Voltage of CdSe cell

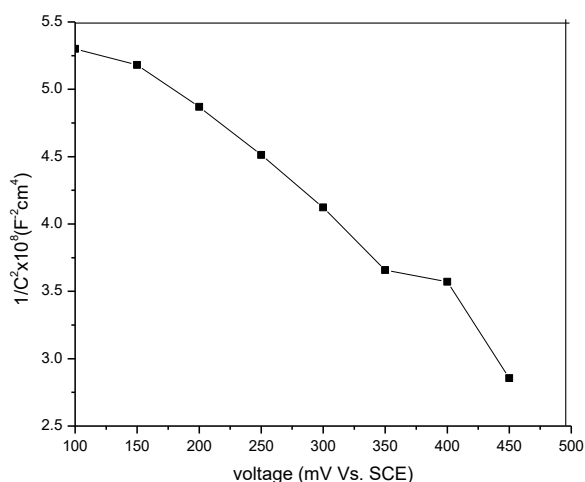


Figure 3: Plot of $1/C^2$ against Voltage of CdSe cell

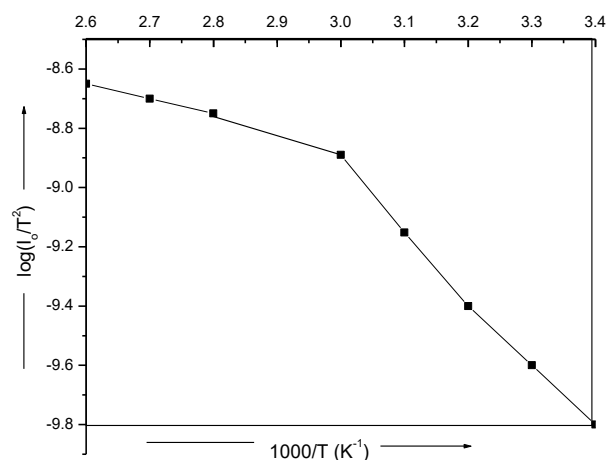


Figure 4: Plot of $\log(I_0/T^2)$ vs $1000/T$ (K^{-1}) of CdSe cell

3.1.3. Barrier-height measurement

The Built-in-Potential, sometimes called barrier-height or ϕ_B , was determined by measuring the reverse saturation current (I_0) passing through the junction at different temperatures between 363 and 303 K. The reverse saturation current passing through the connection is temperature-dependent, per [23]: $I_0 = AT^2 \exp(-\phi_B/kT)$ (1), where k is the Boltzmann constant, A is the Richardson constant, and ϕ_B is the barrier height in eV. The reverse saturation current exhibits an exponential temperature change. $\log(I_0/T^2)$ vs $1000/T$ graphs for the CdSe sample are displayed in figure 4. The slope of the linear section of the plots was used to calculate the photoelectrode's built-in potential values.

3.1.4 Power output characteristics

Figure 6 shows the solar power generation parameters of several cells under 30 mW/cm^2 light intensity. The fill factor (ff), series resistance (R_s), conversion efficiency (η), shunt resistance (R_{sh}), open circuit voltage (V_{oc}), short-

circuit current (I_{sc}), and series resistance (R_s) were among the various cell metrics that were assessed. The open circuit voltage and short-circuit current are found to be 260 mV and 161 $\mu\text{A}/\text{cm}^2$, respectively. The calculations show that the fill factor is 48.11% and the conversion efficiency is 0.64%. Band gap and flat band potential value are both more positive, improving power efficiency. The large short circuit current was caused by increased material absorbance and decreased photoelectrode resistance. The improvement in open circuit voltage was due to an increase in flat band potential. The low efficiency of the inquiry may be due to the high series resistance of the PEC cell, the thin film, and the interface states that drive the recombination process [24]. The values of R_s and R_{sh} were found to be 826 and 543, respectively. The main drawback of employing PEC cells is the lack of a space charge zone at the photoelectrode-electrolyte interface. In this case, the photogenerated charge carriers can go in both directions. The photogenerated electrons in n-type material either quickly recombine with holes or leak out into the electrolyte instead of going through an external circuit, according to Rajeshwar *et al.* [25].

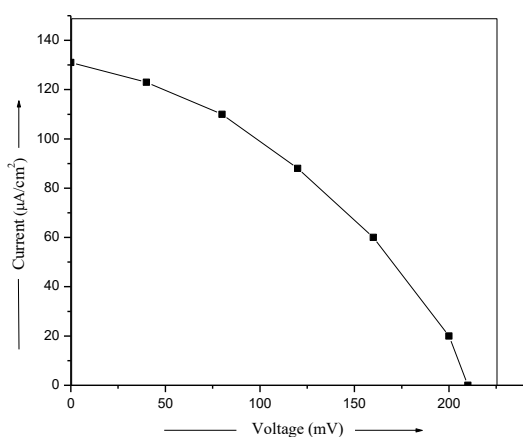


Figure 5: Power Output curves for CdSe Photoelectrode

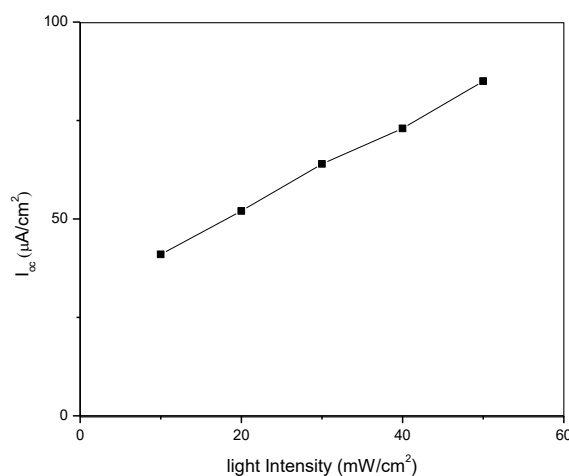


Figure 6: Plot of I_{oc} ($\mu\text{A}/\text{cm}^2$) vs light Intensity (mW/cm^2) of CdSe cell

3.2. Optical proprieties

3.2.1. Photoresponse

We measured the short circuit current and open circuit voltage in relation to light intensity. Figure 6 shows how I_{sc} varies with light intensity, while Figure 7 shows how V_{oc} varies with light intensity. The photoresponse experiments showed that the open circuit voltage changed logarithmically with the incoming light's intensity. However, the observed saturation in open circuit voltage at higher intensities is caused by charge transfer, electrolyte interface saturation, and the non-equilibrium distribution of electrons and holes in the photoelectrode's space charge region. On the other hand, short circuit current travels almost straight.

Plotting $\log I_{sc}$ versus V_{oc} should result in a straight line, and the slope of the line can be used to determine the illuminated ideality factor. The plot of $\log I_{sc}$ against V_{oc} for a sample CdSe photoelectrode is shown in Figure 8. The composition of the CdSe photoelectrode was found to be virtually straight after the junction ideality factor was calculated. Plotting $\log I_{sc}$ versus V_{oc} should result in a straight line, and the slope of the line can be used to determine the illuminated ideality factor. The plot of $\log I_{sc}$ against V_{oc} for a sample CdSe photoelectrode is shown in Figure 8.

The composition of CdSe was found to have the lowest value when the junction ideality factor for each photoelectrode was calculated and shown in Table -1.

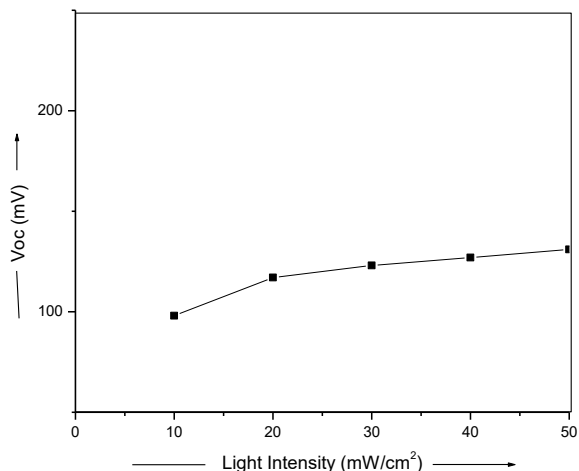


Figure 7: Plot of V_{oc} vs light Intensity of CdSe cell

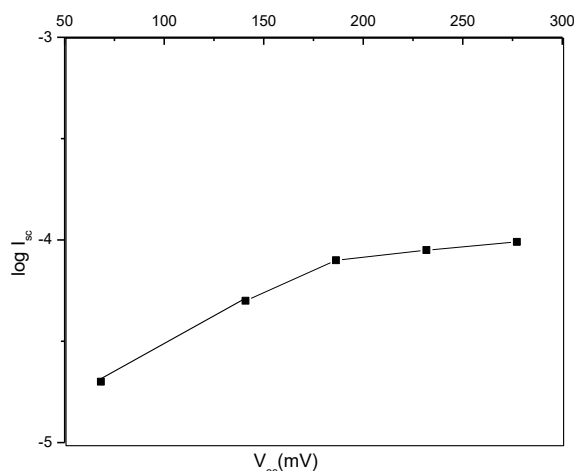


Figure 8: Log I_{sc} vs V_{oc} for CdSe thin film cells

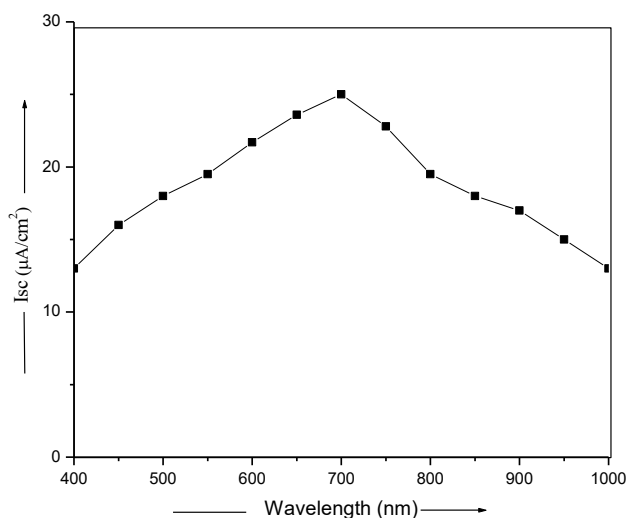


Figure 9: Plot of photocurrent action spectra CdSe thin film cells

Table 1: Photovoltaic and diode parameters obtained from J-V characteristics

V _{oc} mV	I _{sc} µA/cm ²	ff	% efficiency	φ _B	V _{fb}	R _{sh} , Ω	R _s , Ω	n _L	n _d
210	141	43.08	0.35%	0.231	541	651	981	5.49	4.85

3.2.2. Spectral response

Examining the photoelectrochemical cell's spectrum response is one of the best methods to determine its efficacy qualitatively. As a result, the 400–1000 nm wavelength range has been used to assess a cell's spectrum response. Figure 9 shows the photocurrent action spectra following analysis. The spectra for CdSe show that the current decreases with increasing wavelength and reaches its maximum value at about 718 nm. The decrease in current on the shorter wavelength side could be caused by high surface recombination of photogenerated minority carriers and light absorption in the electrolyte. The decrease in current on the longer wavelength side may be due

to the non-optimized thickness and the transition between defect levels. The greatest current, which corresponds to ≈ 718 nm, yields band gap values of 1.71 eV for CdSe, which is consistent with the results of optical absorption experiments. Table-1 lists the PEC cell parameters for the CdSe photoelectrode, including V_{oc} , I_{sc} , %, ff%, V_{fb} , R_s , R_{sh} , n_L , and n_d .

Conclusion

The photoelectrochemical cell is easy to build using a CdSe photoelectrode, sulphide-polysulphide electrolyte, and a CoS-coated graphite rod as a counter electrode. A saturated calomel electrode served as the reference electrode. The various performance indicators were determined with respect to the composition parameter (x). The composition with the highest efficiency and fill factor is found to be CdSe. Maximum open circuit voltage, maximum short circuit current, high flat band potential, and low resistance are the causes of this. The barrier height was examined using the reverse saturation current's temperature dependence. It was discovered that the CdSe photoelectrode had the lowest illuminated ideality factor. This kind of photoelectrode produced a cell with a wider spectrum response and a strong short circuit current.

Acknowledgements

The author would like to thank Prof. J. B. Yadav, Head of the Department, USIC, for providing XRD facilities. The author is also grateful to Dr. Rahul Patil for his moral support. Sincere thanks are extended to Principal Dr. Madhav Bapat, D.B.J. College (Autonomous), Chiplun, for his constant encouragement and moral support in pursuing this research work.

References

1. Musa, A. O., Alkomolate, T., & Carter, M. J. (1998). *Solar Energy Materials and Solar Cells*, 51, 305–310.
2. Becquerel, E., & Senac, C. R. (1839). *Comptes Rendus de l'Académie des Sciences de Paris*, 9, 361–365.
3. Miller, B., Heller, A., Robins, M., Menezes, S., Chang, K. C., & Thomson, J. J. (1977). *Journal of Electrochemistry*, 50, 1019–1024.
4. Aruchami, A., Arvamuda, G., & Subbarao, G. V. (1982). *Bulletin of Materials Science*, 4, 483–489.
5. Chandra, S. (1985). Photoelectrochemical solar cells. In D. S. Campbell (Ed.), *Photoelectrochemical solar cells*. New York, NY: Gordon and Breach Science Publishers.
6. Kalyanasundaram, K. (1985). *Solar Cells*, 15, 93–102.
7. Chandra, S., & Pandya, R. K. (1980). *Physica Status Solidi (a)*, 59, 787–792.
8. Williams, R. (1967). *Journal of the Electrochemical Society*, 114, 1173–1178.
9. Sharon, M. (1986). Photoelectrochemical solar cells. In K. S. V. Santhanam & M. Sharon (Eds.), *UNESCO Training Workshop Proceedings* (p. 6).
10. Chopra, K. L., & Das, S. R. (1983). *Thin film solar cells*. New York, NY: Plenum Press.
11. Shanthi, E., Banerjee, A., Dutta, V., & Chopra, K. L. (1982). Electrical and optical properties of tin oxide films doped with F and (Sb+F). *Journal of Applied Physics*, 53, 1615–1621.
12. Deshmukh, L. P. (1985). *Ph.D. thesis*. Shivaji University, Kolhapur, Maharashtra, India.
13. Shahane, G. S. (1997). *Ph.D. thesis*. Shivaji University, Kolhapur, Maharashtra, India.
14. Mane, S. T., Lendave, S. A., Pingale, P. C., Suryawanshi, R. V., Karande, V. S., Pirgonde, B. R., & Deshmukh, L. P. (2011). In *Proceedings of the International Conference on Advanced Materials and Nanoparticles* (October 21–23). Kathmandu, Nepal.

15. Lendave, S. A., Karande, V. S., & Deshmukh, L. P. (2010). Crystallographic and microscopic investigations on chemically synthesized mercury cadmium sulphide thin composite films. *Journal of Surface Engineering and Applied Electrochemistry*, 46, 462–468.
16. Manificier, J. C., Szepessy, L., Bresse, J. F., Perotin, M., & Struck, R. (1979). $\text{In}_2\text{O}_3:(\text{Sn})$ and $\text{SnO}_2:(\text{F})$ films—Application to solar energy conversion: Part I—Preparation and characterization. *Materials Research Bulletin*, 14, 109–118.
17. More, P. D., Shahane, G. S., Bosale, P. N., Belhekar, A. A., Dongare, M. K., & Deshmukh, L. P. (2002). Micro-crystallographic and spectral response studies of $\text{CdSe}_{1-x}\text{Te}_x$ alloyed thin films. *Indian Journal of Pure and Applied Physics*, 40, 62–67.
18. Abou Sekkina, M. M., Tawfik, A., & Abd El-Ali, M. I. (1985). Further studies on the temperature dependence of the electric and photovoltaic properties of CdSe thin films for solar cells. *Thermochimica Acta*, 86, 59–65.
19. Tembhurkar, Y. D., & Hirde, J. P. (1992). Structural, optical and electrical properties of spray pyrolytically deposited films of copper indium diselenide. *Thin Solid Films*, 215, 65–70.
20. Orton, J. W., & Powell, M. J. (1980). The Hall effect in polycrystalline and powdered semiconductors. *Reports on Progress in Physics*, 43, 1263–1307.
21. Oumous, & Hadiri, H. (2001). Optical and electrical properties of annealed CdS thin films obtained from a chemical solution. *Thin Solid Films*, 386, 87–92.
22. Mott, N. F. (1969). *Philosophical Magazine*, 19, 835–852.
23. Soliman, L. I. (1994). Influence of γ -irradiation on optical and electrical properties of amorphous CuInSeTe, CuInSTe and CuInSeS thin films. *Indian Journal of Pure and Applied Physics*, 32, 166–172.
24. Suzuki, T., Ema, Y., & Toshiya, H. (1987). Indium doping in CdTe film by co-evaporation of CdTe and In. *Japanese Journal of Applied Physics*, 26, 2009–2014.
25. Pujari, V. B., Dhage, D. J., & Deshmukh, L. P. (2008). n- $\text{Hg}_x\text{Cd}_{1-x}\text{Se}$ thin film electrodes for photoelectrochemical applications. *Indian Journal of Engineering & Materials Science*, 15, 275–281.